

Ground-state structure of the hydrogen double vacancy on Pd(111)

Sungho Kim and Seong-Gon Kim*

*Department of Physics and Astronomy, Mississippi State University, Mississippi State, MS 39762, USA and
Center for Advanced Vehicular Systems, Mississippi State University, Mississippi State, MS 39762, USA*

S. C. Erwin

Center for Computational Materials Science, Naval Research Laboratory, Washington, DC 20375, USA

(Dated: June 26, 2007)

We determine the ground-state structure of a double vacancy in a hydrogen monolayer on the Pd(111) surface. We represent the double vacancy as a triple vacancy containing one additional hydrogen atom. The potential-energy surface for a hydrogen atom moving in the triple vacancy is obtained by density-functional theory, and the wave function of the fully quantum hydrogen atom is obtained by solving the Schrödinger equation. We find that an H atom in a divacancy defect experiences significant quantum effects, and that the ground-state wave function is centered at the hcp site rather than the fcc site normally occupied by H atoms on Pd(111). Our results agree well with scanning tunneling microscopy images.

PACS numbers: 31.15.es, 61.72.jd, 68.43.Fg,

I. INTRODUCTION

Understanding the fundamental mechanisms that govern the behavior of hydrogen on metal surfaces is important to new technologies involving hydrogen production, storage, and energy conversion^{1,2,3,4}. Because of its light mass, hydrogen can manifest uniquely quantum effects not seen for other elements. These effects can have striking consequences when the dimensionality of the allowed motion is constrained by adsorption on a surface^{5,6,7,8,9,10}. When a metal surface such as palladium is covered by a nearly complete monolayer of hydrogen, small clusters of vacancies in the hydrogen layer serve as active sites for the dissociative adsorption of additional H₂ molecules^{11,12}. Despite their central role in catalysis, the exact nature of these vacancy defects is not well understood.

It has been generally accepted that the dissociative adsorption of the diatomic molecule H₂ is to require at least two adjacent and empty atomic adsorption sites (or vacancies) based on early studies of Langmuir^{11,13}. Recently, intriguing observations about hydrogen divacancies on palladium were made using scanning tunneling microscopy (STM). Mitsui and co-workers^{14,15} reported that hydrogen molecules impinging on an almost H-saturated Pd(111) surface did not adsorb in two-vacancy sites. Rather, aggregates of three or more hydrogen vacancies were required for efficient dissociation of H₂ molecules. These findings led to speculations that the standard description from Langmuir adsorption kinetics¹¹ might be too simple to explain the dissociative adsorption of hydrogen on Pd(111)^{12,14,15,16}.

However, Groß and Dianat have recently shown, using *ab initio* molecular dynamics (AIMD) simulations, that no change in the original Langmuir picture is warranted¹⁷. Based on more than 4000 AIMD trajectories, Groß *et al.* unambiguously demonstrated that a divacancy is still sufficient to dissociate hydrogen molecules

provided the kinetic energy of the incident molecules is large enough to overcome the relatively small energy barrier. For an initial kinetic energy of 0.02 eV, roughly corresponding to the kinetic energy of the H₂ molecules in Mitsui's experiment, no dissociative adsorption events were observed on the almost hydrogen-covered Pd(111) surface, thus confirming the experimental findings. When the initial kinetic energy was increased to 0.1 eV so that the small barrier found for H₂ on Pd(111) at high coverage¹⁶ can be overcome, a nonvanishing adsorption probability was observed.

To further improve our understanding of dissociative adsorption of H₂ on Pd(111), an accurate description of the ground-state structure of the double vacancy in a hydrogen monolayer on the surface is desirable. Mitsui *et al.*^{14,15} found that divacancies have a triangular STM image extending over three neighboring sites, instead of a linear image over two neighboring sites. In this paper, by determining the ground-state structure of the divacancy in a hydrogen monolayer on Pd(111), we show theoretically that the quantum nature of the H atom accounts for the observed STM imagery. Our findings indicate that the quantum wave nature of hydrogen motion provides a simple and elegant foundation to the traditional classical explanations for such observations^{12,16,18}, and suggest that the quantum nature of hydrogen may play a surprisingly prominent role in other similarly confined systems.

II. METHODS

Fig. 1 shows a schematic representation of several simple hydrogen vacancy configurations on Pd(111) considered in the present work. A double vacancy can be considered as a single H atom (red circles in Fig. 1) moving in the triangular area formed by $3V_H$. As noted by Mitsui *et al.*, this H atom is much more mobile than all

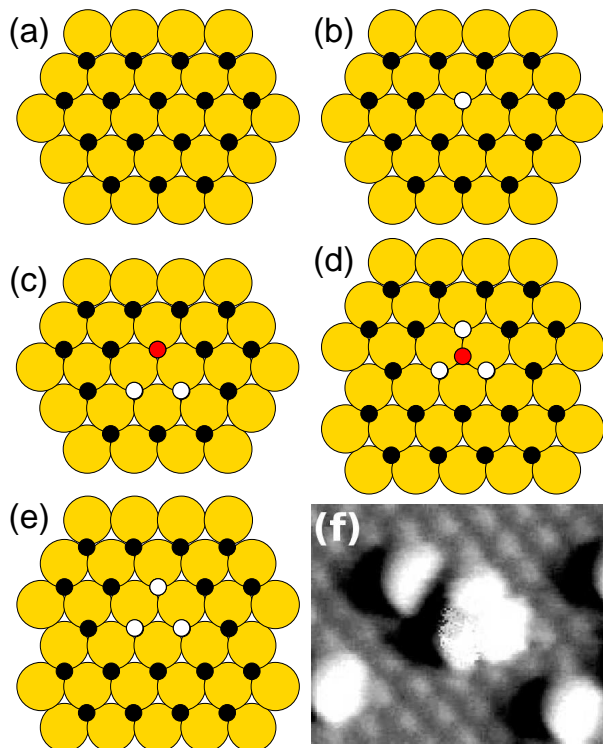


FIG. 1: (color online) Hydrogen vacancy configurations: (a) fully hydrogenated Pd(111) surface; (b) single vacancy, $1V$; (c) classical model for a divacancy, $2V_c$; (d) ground-state configuration of the quantum mechanical divacancy, $2V_q$; (e) trivacancy centered around a hcp site, ($3V_H$). Pd atoms are represented by large gold circles and H atoms by smaller black circles. The white circles represent empty fcc sites while the red circle represents a H atom that moves in the triangular area formed by $3V_H$. (f) An STM image of a divacancy. Reprinted from Ref. 14 with permission.

other H atoms that form $3V_H$.^{14,15} Previous models that treated H atoms classically considered only $2V_c$ where the (red) H atom hops among three fcc sites via thermal diffusion.¹⁴ As we will show later, however, full quantum treatment of the mobile H atom reveals that the ground-state configuration for divacancy is $2V_q$ where the central H atom occupies the hcp site rather than fcc sites. Exchange with the H atoms forming the walls of the triangle of $3V_H$ requires hopping near top Pd sites and/or close to other H atoms, a process with a higher barrier and therefore much slower than the motion of the H atom *in* the vacancy. Hence, the problem of determining the minimum energy configuration of a divacancy is equivalent to solving the Schrödinger equation for a single hydrogen atom moving in the external potential of hydrogen and palladium atoms having the $3V_H$ configuration.

Within the Born-Oppenheimer approximation¹⁹, the Schrödinger equation for the motion of a hydrogen atom with mass M is

$$-\frac{\hbar^2}{2M}\nabla^2\psi(\mathbf{r}) + U(\mathbf{r})\psi(\mathbf{r}) = E\psi(\mathbf{r}). \quad (1)$$

The 3-dimensional potential energy surface (PES), $U(\mathbf{r})$, contains the contributions to the total energy from all Pd atoms in the slab, all hydrogen atoms adsorbed on the surface, and the hydrogen atom in question at \mathbf{r} . When only the position of this hydrogen atom is varied, $U(\mathbf{r})$ becomes, in effect, the potential energy surface for its motion.

The PES was mapped out by calculating the adsorption energy of the hydrogen atom placed at different positions over a $3V_H$ defect. We formed the defect within a periodic 3×3 surface unit cell, which is large enough to prevent significant interaction with periodic images in neighboring cells. The potential energy surface was sampled according to the importance of each region: sample points were densely distributed near points of interest such as the fcc sites, the hcp sites, and along the pathway between them, while points far from these locations were sampled less densely. Altogether over 3500 energy points were evaluated, distributed within about 60 planes parallel to the surface and separated by 0.1 \AA .

All *ab initio* total-energy calculations and geometry optimizations are performed within density functional theory (DFT)^{20,21} using ultrasoft pseudopotentials (USPP)²² as implemented by Kresse et. al.^{20,23} Exchange-correlation effects were treated within the local-density approximation (LDA)^{24,25}. The electron wave functions were expanded in a plane-wave basis set with cutoff energy 250 eV. The resulting equilibrium lattice constant of bulk Pd was 3.86 \AA in excellent agreement with the experimental value of 3.89 \AA ²⁶. We used a standard supercell technique to model the Pd(111) surface as slabs of four Pd layers separated by 12 \AA of vacuum. The surface Brillouin zone was sampled using a 6×6 Monkhorst-Pack k -point set. Structural optimization was performed until the energy difference between successive steps was less than 1 meV. After applying a well-known correction for the LDA binding energy of H_2 ²⁷, we obtained the hydrogen adsorption energy $E_{ad}=0.46 \text{ eV}$, in excellent agreement with the experimental value of 0.45 eV ²⁸. Based on tests performed with thicker slabs and larger vacuum gaps, we estimate the uncertainty in this energy to be roughly 0.02 eV. Tests using the generalized-gradient approximation (GGA)²⁹ show that E_{ad} values for different sites shift rigidly. This would have no effect on our main results below, because the PES depends only on differences in adsorption energies, which are unchanged.

We solved the Schrödinger equation (1) numerically in momentum space. Although we are modeling a hydrogen atom moving in an isolated $3V_H$ defect, we nonetheless use periodic boundary conditions in order to take advantage of Bloch's theorem and the convenience of using plane waves as a basis. To minimize computational requirements, we used a unit cell with the full C_{3v} symmetry of the underlying lattice.

The wave functions for the hydrogen atom are expanded in a plane-wave basis with a cutoff energy of 0.3 eV, which is equivalent to a cutoff of roughly 550 eV

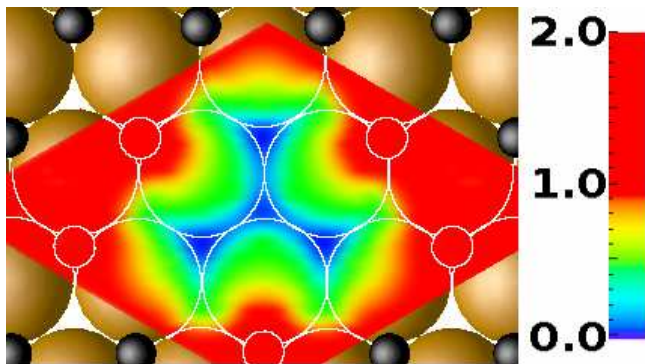


FIG. 2: (color online) Minimum potential energy surface for a hydrogen atom in a divacancy. The minimum potential energy in the z -direction for all points in the xy -plane of a single classical H atom moving in a three site cluster. Large and small white circles representing top layer Pd atoms and neighboring H atoms, respectively, are drawn as visual guides. The color bar shows corresponding potential values in eV.

for electronic band-structure calculations. Our tests show that the eigenvalues of the hydrogen-atom wave functions are well converged with this cutoff. Since we simulate an isolated $3V_H$ defect with a large unit cell, the Brillouin zone is very small, and hence k point sampling is not important. The eigenvalues for different k points exhibit very little dispersion, and therefore we use just a single k -point at the zone center. Finally, the wave functions are well confined inside the potential well, with no significant tailing outside the boundaries of the potential well, indicating that the 3×3 surface unit cell is adequate.

III. RESULTS

Fig. 2 shows the minimum PES for a hydrogen atom in a $3V_H$ defect. Two important conclusions can be drawn from this energy surface. First, the only low-energy pathways available to the hydrogen atom are those connecting the three fcc sites to central hcp site. Second, there are no low-energy pathways available to allow the surrounding hydrogen atoms to move into the vacancy region. The region of low potential (blue and green) is surrounded by neighboring H atoms and by construction possesses C_{3v} symmetry about the central hcp site. The potential floor (blue) region has three branches extending from the central hcp site to fcc sites, where the potential reaches its minimum. The local minimum at the hcp site is 20 meV higher than at the fcc sites.

The results of our calculations for the low-energy eigenstates are summarized in Table I, and their wavefunctions are shown in Fig. 3. Of particular interest is the ground state ($1A_1$), which is localized at the hcp site. We note that this is not the minimum of the potential-energy surface (which occurs at the fcc sites). If the H atom had been treated classically, the ground state configuration

TABLE I: The energies of eigenstates for a H atom in a divacancy. The potential energies are measured from the bottom of the potential. Difference in energies are measured from those of the ground state ($1A_1$). States $2A_1$, $1E_1$, and $1E_2$ are considered to be degenerate. All energy values are given in meV.

Index	state	E_{tot}	E_{kin}	E_{pot}	ΔE_{tot}	ΔE_{kin}	ΔE_{pot}
1	$1A_1$	177	68	109	–	–	–
2	$2A_1$	191	72	119	14	4	10
3	$1E_1$	192	71	121	15	3	12
4	$1E_2$	193	71	122	16	3	13
5	$2E_1$	245	78	167	68	10	58

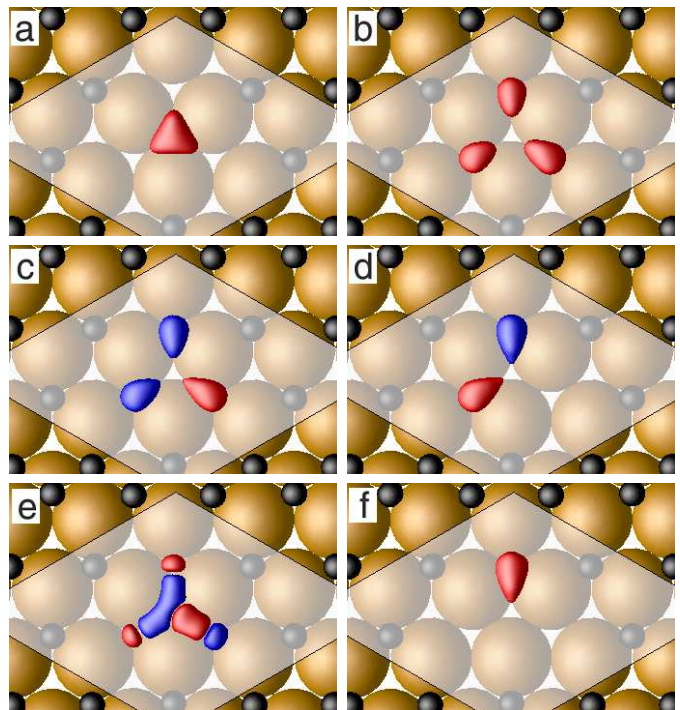


FIG. 3: (color online) Wave functions of a H atom in a divacancy. Isosurface of the real component of the wave functions of a hydrogen atom in a structure used to simulate a $2V_a$ vacancy defect that contains three fcc sites and one hcp site. The isovalues on red surfaces are positive while the values on blue surfaces are negative. All imaginary components are zero. (a) The ground state, ϕ_{1A_1} . The red surface contains 99.3% of the total integrated probability (TIP). (b) The first excited state, ϕ_{2A_1} . Three red surfaces contain 99.1% of the TIP. (c) One of the first doublet excited states, ϕ_{1E_1} . The red surface contains 58.7% of the TIP while two blue surfaces contain 40.3%. (d) The other first doublet excited states, ϕ_{1E_2} . Each surface contains 49.6% of the TIP. (e) One of the second doublet excited states, ϕ_{2E_1} . The red surface contains 61.4% of the TIP while two blue surfaces contain 37.5%. (f) One of the mixed states delocalized over an fcc site: $\Psi_{\text{fcc}} = \frac{1}{\sqrt{6}}(\sqrt{2}\phi_{2A_1} - \phi_{1E_1} - \sqrt{3}\phi_{1E_2})$. The red surface contains 99.4% of the TIP.

would have the H atom adsorbed at the fcc site, corresponding to the defect configuration $2V_c$.

To understand better the origin of this quantum effect we list separately, in Table I, the kinetic- and potential-energy contributions to the total energy. Our result indicates that the quantum-mechanical shift is driven by both the kinetic and potential energy of the hydrogen-atom wave function. Even though the minimum potential at the hcp site is slightly higher than that of three fcc sites, the potential well at the hcp site is wider than those at the fcc sites. By localizing around the central hcp site, the ground-state wave function can sufficiently lower its potential energy (by reducing the penetration of wave function into the region of higher potential) and kinetic energy (by reducing the gradient of the wave function) to compensate the small increase of potential around the hcp site. Hence, the fully quantum mechanical ground-state geometry for the hydrogen divacancy is not the classical configuration $2V_c$ of Fig. 1(c), but rather the quantum configuration $2V_q$ illustrated in Fig. 1(d). Indeed, in order to realize a configuration similar to the classical $2V_c$, the quantum wave function must be localized on one of the fcc sites as shown Fig. 3(e). This requires constructing, at the cost of 14 meV, a linear combination three degenerate excited states: $\Psi_{fcc} = \frac{1}{\sqrt{6}}(\sqrt{2}\phi_{2A_1} - \phi_{1E_1} - \sqrt{3}\phi_{1E_2})$.

IV. DISCUSSION

One prediction that arises from this fully quantum-mechanical calculation is that the ground-state of the hydrogen quantum divacancy $2V_q$ will have intrinsically triangular symmetry, suggesting that STM images should appear triangular as well. Because it is locally insulating, an adsorbed hydrogen atom screens the tunneling current between the STM tip and the metal substrate. Thus, a site occupied by an hydrogen atom has a low apparent height (dark in a standard STM representation) while a vacancy appears high (bright)¹⁴. As a result, *a divacancy is expected to appear as a three-lobed object with triangular symmetry*. Recent STM images, reproduced

in Fig. 1(f), confirm this behavior^{14,15}. Alternative explanations based on classical thermal diffusion^{14,15}, although consistent with the observed symmetry, are not necessary to explain such images. For the trivacancy and larger multi-vacancy defects, the quantum effects manifested in the divacancy are suppressed and the delocalized H atoms behave more like classical particles. In these cases, thermal diffusion provides a reasonable explanation for the observed STM imagery^{14,15}.

Our results also suggest that future studies involving divacancies of H atoms on metal (111) surfaces need to include the quantum configuration $2V_q$ shown in Fig. 1(d) as one of the viable stable configurations even if the total energy of the structure when H atoms are treated classically is somewhat higher.

V. CONCLUSIONS

We have studied the quantum nature of hydrogen atoms on Pd(111) surface by solving the Schrödinger equation for an H atom moving in static potential energy surface determined from first-principles density-functional theory calculations. We find that a H atom in a divacancy defect experiences significant quantum effects, with the result that its wave functions are extended over large portion of the vacancy. The ground-state H wave function is centered at an hcp site rather than the fcc site occupied by classical H atoms. As a result, the divacancy should exhibit a triangular geometry with three-fold symmetry, consistent with recent experiments.

VI. ACKNOWLEDGMENT

This work was in part supported by the Department of Defense under the CHSSI MBD-04 (Molecular Packing Software for *ab initio* Crystal Structure and Density Predictions) project and by the Office of Naval Research. Computer time was provided by the High Performance Computing Collaboratory (HPC²) at Mississippi State University.

* Electronic address: kimsg@ccs.msstate.edu

¹ G. W. Huber, J. W. Shabaker, and J. A. Dumesic, *Science* **300**, 2075 (2003).

² L. Schlappbach and A. Züttel, *Nature* **414**, 353 (2001).

³ B. C. H. Steele and A. Heinzl, *Nature* **414**, 345 (2001).

⁴ S. G. Chalk, J. F. Miller, and F. W. Wagner, *J. Power Sources* **86**, 40 (2000).

⁵ L. Lauhon and W. Ho, *Phys. Rev. Lett.* **85**, 4566 (2000).

⁶ G. X. Cao, E. Nabighian, and X. D. Zhu, *Phys. Rev. Lett.* **79**, 3696 (1997).

⁷ X. D. Zhu, A. Lee, and A. Wong, *Phys. Rev. Lett.* **68**, 1862 (1992).

⁸ G. Källén and G. Wahnström, *Phys. Rev. B* **65**, 033406 (2001).

⁹ A. Gross, *Surf. Sci.* **363**, 1 (1996).

¹⁰ L. Y. Chen and S. C. Ying, *Phys. Rev. Lett.* **73**, 700 (1994).

¹¹ H. Conrad, G. Ertl, and E. E. Latta, *Surf. Sci.* **41**, 435 (1974).

¹² S. Holloway, *Surf. Sci.* **540**, 1 (2003).

¹³ I. Langmuir, *J. Am. Chem. Soc.* **38**, 1145 (1916).

¹⁴ T. Mitsui, M. K. Rose, E. Fomin, D. F. Ogletree, and M. Salmeron, *Nature* **422**, 705 (2003).

¹⁵ T. Mitsui, M. K. Rose, E. Fomin, D. F. Ogletree, and M. Salmeron, *Surf. Sci.* **540**, 5 (2003).

¹⁶ N. Lopez, Z. Lodziana, F. Illas, and M. Salmeron, *Phys.*

- Rev. Lett. **93**, 146103 (2004).
- ¹⁷ A. Gross A, A. Eichler, J. Hafner, M. J. Mehl, and D. A. Papaconstantopoulos, Surf. Sci. **539**, L542 (2003).
- ¹⁸ B. Hammer, Phys. Rev. B **63**, 205423 (2001).
- ¹⁹ Ira N. Levine, *Quantum Chemistry* (Prentice-Hall, Upper Saddle River, New Jersey, 2000).
- ²⁰ G. Kresse and J. Furthmüller, Phys. Rev. B **54**, 11169 (1996).
- ²¹ W. Kohn and L. J. Sham, Phys. Rev. **140**, A1133 (1965).
- ²² D. Vanderbilt, Phys. Rev. B **41**, 7892 (1990).
- ²³ G. Kresse and J. Hafner, J. Phys.: Cond. Matt. **6**, 8245 (1994).
- ²⁴ D. M. Ceperley and B. J. Alder, Phys. Rev. Lett. **45**, 566 (1980).
- ²⁵ J. P. Perdew and A. Zunger, Phys. Rev. B **23**, 5048 (1981).
- ²⁶ C. Kittel, *Introduction to Solid State Physics* (Addison-Wesley, Reading, MA, 1986).
- ²⁷ W. Dong, G. Kresse, J. Furthmüller, and J. Hafner, Phys. Rev. B **54**, 2157 (1996).
- ²⁸ K. Christmann, G. Ertl, and D. Schober, Surf. Sci. **40**, 61 (1973).
- ²⁹ J. P. Perdew, K. Burke, and M. Ernzerhof, Phys. Rev. Lett. **77**, 3865 (1996).